Silicon−Carbon Unsaturated Compounds. 72. Thermolysis of Acylpolysilanes with Diphenylketene

Akinobu Naka,[†] Nana Fujioka,[†] Joji Ohshita,[‡] Junnai Ikadai,[‡] Atsutaka Kunai,[‡] Hisayoshi Kobayashi,*[,#] Toshiko Miura,[#] and Mitsuo Ishikawa*[,†]

Department of Life Science, Kurashiki University of Science and the Arts, 2640 Nishinoura, Tsurajima-cho, Kurashiki, Okayama 712-8505, Japan, Department of Applied Chemistry, Graduate School of Engineering, Hiroshima University, Higashi-Hiroshima 739-8527, Japan, and Department of Chemistry and Materials Technology, Kyoto Institute of Technology, Matsugasaki, Kyoto 606-8585, Japan

Received August 19, 2007

The thermolysis of pivaloyl- and adamantoyltris(trimethylsilyl)silane (**1** and **2**) with diphenylketene in a sealed glass tube at 140 °C for 24 h afforded 2-*tert*-butyl- and 2-adamantyl-1,1-dimethyl-3-[methylbis-(trimethylsiloxy)silyl]-4,4-diphenyl-1-silacyclobut-2-ene (**6** and **7**) in 44% and 50% isolated yields, respectively. Related thermolysis of mesitoyltris(trimethylsilyl)silane (**3**) with diphenylketene at 160 °C for 24 h, however, proceeded with high stereospecificity to give *cis*-3-diphenylmethylene-4-mesityl-2-trimethylsiloxy-2,4-bis(trimethylsilyl)-2-siloxetane (**8**) in 44% yield. When **8** was heated at 200 °C for 24 h, 1-mesityl-3,3-diphenyl-1-(trimethylsilyl)propadiene was obtained in 43% yield. Computational analyses for the formation of siloxetanes arising from addition of silenes to ketene and succesive isomerization of the siloxetanes thus formed, leading to the products, are described. The results of X-ray crystallographic analysis for the product **6** formed by the co-thermolysis of **1** and diphenylketene are reported.

Introduction

In the past decade, the reactions of silenes, which are produced by the photolysis,[1] thermolysis,[2,3] and Peterson-type reaction[4] of acylpolysilanes, with various organic compounds have been extensively investigated, and many papers concerning these studies have been published to date. The reactions of the silenes with carbonyl compounds have also been examined, and the siloxetanes are considered to be produced as the intermediates.[5] In fact, in the reactions of the relatively stable silenes with nonenolizable ketones, the [2 + 2] cycloadducts, siloxetanes, have been isolated.[5a] In addition to the siloxetanes, the formation of the [2 + 4] cycloadducts has been observed in some cases.[1c,3a]

We have demonstrated that the co-thermolysis of pivaloyl- and adamantoyltris(trimethylsilyl)silane with acetone affords two types of siloxymethylcyclopropane derivatives and silyl enol ethers, arising from a 1,2-trimethylsiloxy shift from carbon to silicon in the siloxetane intermediates, which are probably produced by formal [2 + 2] cycloaddition of the silenes to a carbonyl group.[3a] Similar thermolysis of the acylpolysilanes with benzophenone, however, gives the products derived from both [2 + 2] and [2 + 4] cycloaddition.[3a]

As a part of our studies concerning the reactions of the silenes generated thermally from acylpolysilanes with carbonyl compounds, we have examined the co-thermolysis of pivaloyl-, adamantoyl-, and mesitoyltris(trimethylsilyl)silane with diphenylketene. We have also carried out computational analyses for these reactions to elucidate the mechanism involving succesive isomerization of the initial adducts, siloxetanes, arising from [2 + 2] cycloaddition of silenes with diphenylketene, leading to the products. For the reaction of the silenes with ketene, the reaction of trimethylsilylketene with the silenes generated photochemically from adamantoyl- and pivaloyltis(trimethylsilyl)silane has been reported by Brook and Baumegger as the sole example.[6]

* Corresponding author. E-mail: ishikawa-m@kcat.zaq.ne.jp.
[†] Kurashiki University of Science and the Arts.
[‡] Hiroshima University.
[#] Kyoto Institute of Technology.

(1) (a) Brook, A. G. *J. Organomet. Chem.* **1986**, *300*, 21. (b) Brook, A. G. In *The Chemistry of Organic Silicon Compounds*, Patai, S., Rappoport, Z., Eds.; Wiley: New York, 1989; Chapter 15. (c) Müller, T.; Ziche, W.; Auner, N. In *The Chemistry of Organic Silicon Compounds*; Rappoport, Z., Apeloig, Y., Eds.; Wiley: New York, 1998; Vol. 2, Chapter 16. (d) Brook, A. G. In *The Chemistry of Organic Silicon Compounds*; Rappoport, Z., Apeloig, Y., Eds.; Wiley: New York, 1998; Vol. 2, Chapter 21. (e) Morkin, T. L.; Leigh, W. J. *Acc. Chem. Res.* **2001**, *34*, 129. (f) Morkin, T. L.; Owens, T. R.; Leigh, W. J. In *The Chemistry of Organic Silicon Compounds*; Rappoport, Z. A., Appeloig, Y., Eds,; Wiley: New York, 2001; Chapter 17.

(2) (a) Brook, A. G.; Harris, J. W.; Lennon, J.; Elsheikh, M. *J. Am. Chem. Soc.* **1979**, *101*, 83. (b) Brook, A. G.; Nyburg, S. C.; Abdesaken, F.; Gutekunst, B.; Gutekunst, G.; Krishna, R.; Kallury, M. R.; Poon, Y. C.; Chan, Y.-M.; Wong-Ng, W. *J. Am. Chem. Soc.* **1982**, *104*, 5667.

(3) (a) Ishikawa, M.; Matsui, S.; Naka, A.; Ohshita, J. *Organometallics* **1996**, *15*, 3836. (b) Naka, A.; Ishikawa, M. Matsui, S.; Ohshita, J.; Kunai, A. *Organometallics* **1996**, *15*, 5759. (c) Naka, A. Ishikawa, M. *J. Organomet. Chem.* **2000**, *611*, 248. (d) Naka, A.; Ikadai, J.; Motoike, S.; Yoshizawa, K.; Kondo, Y.; Kang, S.-Y.; Ishikawa, M. *Organometallics* **2002**, *21*, 2033. (e) Yoshizawa, K.; Kondo, Y.; Kang, S.-Y.; Naka, A.; Ishikawa, M. *Organometallics* **2002**, *21*, 3271.

(4) (a) Brook, A. G.; Chiu, P.; McClenaghnan, J.; Lough, A. J. *Organometallics* **1991**, *10*, 3292. (b) Ohshita, J.; Masaoka, Y.; Ishikawa, M. *Organometallics* **1991**, *10*, 3775; **1993**, *12*, 876. (c) Bravo-Zhivotovskii, D.; Brande, V.; Stanger, A.; Kapon, M.; Apeloig, Y. *Organometallics* **1992**, *11*, 2326. (d) Apeloig, Y.; Bendikov, M.; Yuzefovich, M., Nakash, M.; Bravo-Zhivotovskii, D.; Bläser, D.; Boese, R. *J. Am. Chem. Soc.* **1996**, *118*, 12228. (e) Krempner, C.; Oehme, H. *J. Organomet. Chem.* **1994**, *464*, C7. (f) Krempner, C.; Reinke, H.; Oehme, H. *Angew. Chem., Int. Ed. Engl.* **1994**, *33*, 1615.

(5) (a) Brook, A. G.; Chatterton, W. J.; Sawyer, J. F.; Hughes, D. W.; Vorspohl, K. *Organometallics* **1987**, *6*, 1246. (b) Milnes, K. K.; Baines, K. M. *Organometallics* **2007**, *26*, 2392.

(6) Brook, A. G.; Baumegger, A. *J. Organomet. Chem.* **1993**, *446*, C9.

10.1021/om700838n CCC: $37.00
Publication on Web 10/03/2007

Scheme 1

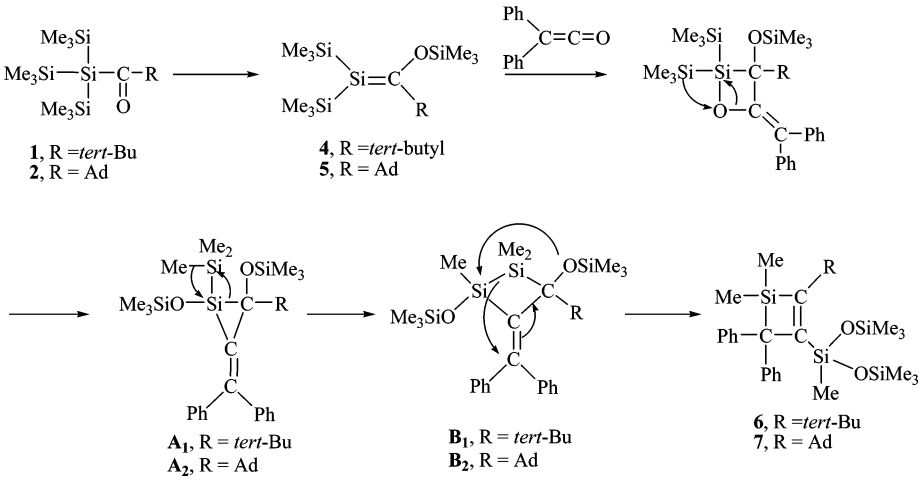

Results and Discussion

When pivaloyltris(trimethylsilyl)silane (**1**) was heated in the presence of 1.2 equiv of diphenylketene in a sealed glass tube at 140 °C for 24 h, 2-*tert*-butyl-1,1-dimethyl-3-[methylbis-(trimethylsiloxy)silyl]-4,4-diphenyl-1-silacyclobut-2-ene (**6**) was obtained in 44% isolated yield, in addition to 50% of the unchanged starting compound **1**, as shown in Scheme 1. The structure of **6** was confirmed by mass and ^{1}H, ^{13}C, and ^{29}Si NMR spectrometric analysis and also by X-ray crystallographic analysis.

The ^{13}C NMR spectrum for **6** shows three signals at −0.42, 1.92, and 2.38 ppm, due to Me_2Si, Me_3SiO, and MeSi carbons, and three signals at 30.82, 36.27, and 52.64 ppm, attributed to the *tert*-butyl carbon atoms and the sp^3-hybridized carbon in the four-membered ring. Olefinic carbons in the silacyclobutene ring appear at 158.14 and 179.54 ppm, respectively, as well as four signals due to the phenyl carbon atoms. Its ^{29}Si NMR spectrum indicates three different kinds of signals at −42.2, 6.6, and 16.9 ppm, due to MeSi, Me_2Si, and Me_3SiO silicons, as expected. An ORTEP representation of the molecular structure for **6** is shown in Figure 1.

The thermal reaction of adamantoyltris(trimethylsilyl)silane (**2**) with diphenylketene under the same conditions gave 2-adamantyl-1,1-dimethyl-3-[methylbis(trimethylsiloxy)silyl]-4,4-diphenyl-1-silacyclobut-3-ene (**7**), analogous to compound **6**, in 50% isolated yield, along with 40% of the unchanged starting compound **2**. The structure of **7** was verified by mass and ^{1}H, ^{13}C, and ^{29}Si NMR spectrometric analysis, as well as by elemental analysis (see Experimental Section). All NMR spectral data obtained for **7** were found to be very similar to those for compound **6**, with the exception of the signals due to the adamantyl group. For example, the ^{29}Si NMR spectrum for **7** reveals three signals at −42.4, 6.5, and 17.2 ppm, attributed to the MeSi, Me_2Si, and Me_3SiO silicon atoms, respectively.

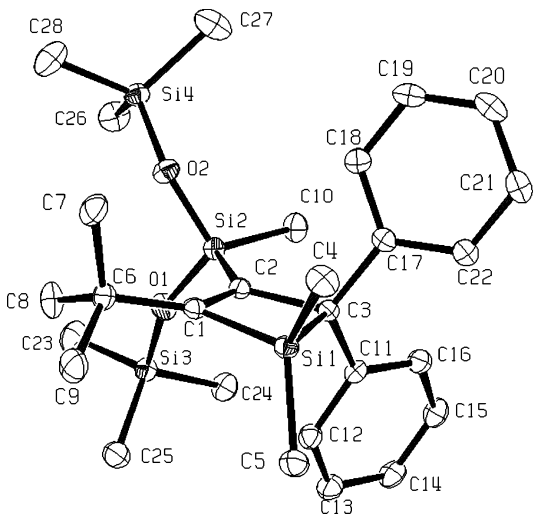

Figure 1. ORTEP diagram for **6** showing thermal ellipsoids at the 50% level. H atoms are omitted for clarity.

It has been reported that the reaction of the silenes generated by the photolysis of **1** and **2** with trimethylsilylketene affords the products, noncyclic acylsilane adducts, derived from the intermediates, in which bonding has occurred between the sp^2-hybridized silicon atom of the silene and the terminal carbon atom of the silylketene.[6] However, the reaction with diphenylketene produced cyclic compounds **6** and **7**, a quite different type of products from those reported by Brook and Baumegger. The formation of the products **6** and **7** may be best understood by the reactions of the silenes **4** and **5** generated thermally from **1** and **2** with diphenylketene. In these reactions, presumably, formal [2 + 2] cycloaddition of the silenes to a carbon−oxygen double bond in diphenylketene takes place to give the siloxetanes, and then the resulting siloxetanes undergo ring contraction to give the silacyclopropane intermediates (**A$_1$** and **A$_2$**). Although we carried out the reactions of **1** and **2** with diphenylketene under various conditions, no siloxetane derivatives were detected in the reaction mixture. A 1,2-methyl shift from the trimethylsilyl group to the ring silicon atom in the silacyclopropanes **A$_{1,2}$** gives the disilacyclobutane intermediates (**B$_1$** and **B$_2$**). Finally, the skeletal rearrangement of **B$_{1,2}$** produces the products **6** and **7**, respectively (Scheme 1).

To our surprise, the co-thermolysis of mesitoyltris(trimethylsilyl)silane (**3**) with diphenylketene in a sealed glass tube at 140 °C for 24 h afforded a different type of product from compounds **6** and **7**, which were obtained in the reaction of **1** and **2** with diphenylketene. In this reaction, *cis*-3-diphenylmethylene-4-mesityl-2-trimethylsiloxy-2,4-bis(trimethylsilyl)-2-siloxetane (**8**) was obtained in 16% yield, along with 76% of the unchanged starting compound **3** (Scheme 2). No *trans*-2-siloxetane isomer was detected in the reaction mixture. Similar treatment of **3** with diphenylketene at higher temperature (160 °C) for 24 h gave **8** in 44% yield, together with 17% of the starting compound **3**. As expected, treatment of **8** in a sealed tube at 200 °C for 24 h produced 1-mesityl-2,2-diphenyl-1-trimethylsilylpropadiene (**9**) in 43% yield. The cyclic trimer of

Scheme 2

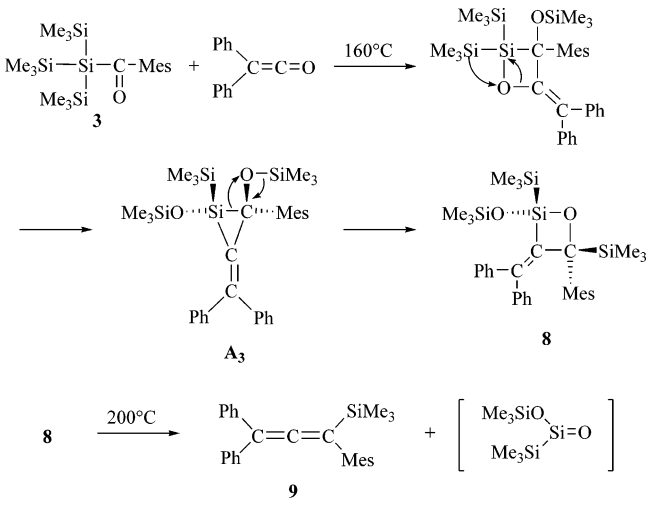

trimethylsiloxy(trimethylsilyl)silanone was also detected in the reaction mixture by high-resolution mass spectrometric analysis.

We have carried out X-ray crystallographic analysis to confirm the structure of **8** several times, with the use of the crystals obtained from the different kinds of solvents; however, all attempts to solve the structure of this compound were unsuccessful. Therefore, its structure was verified by mass and ^{1}H, ^{13}C, and ^{29}Si NMR spectrometric analysis, as well as by elemental analysis. The ^{1}H NMR spectrum for **8** indicates the presence of three kinds of trimethylsilyl protons, three nonequivalent methyl protons for the mesityl group, and aromatic ring protons. Its ^{13}C NMR spectrum shows three signals at −1.46, −0.94, and 1.10 ppm due to trimethylsilyl carbons and three resonances at 20.45, 21.72, and 23.65 ppm attributable to methyl carbons, together with 14 signals attributed to the sp^{2}-hybridized carbon atoms. The signal at 96.68 ppm, due to sp^{3}-hybridized carbon in the siloxetane ring, clearly indicates that the oxygen atom attaches to this carbon.

The ^{1}H−^{29}Si COSY NMR spectrum of **8** reveals that the trimethylsiloxy protons at −0.16 ppm couple with the silicon atom at 11.8 ppm, while the trimethylsilyl protons at −0.07 ppm couple with two silicon atoms at −19.1 and 2.6 ppm, due to the ring silicon and trimethylsilyl silicon. Similarly, the trimethylsilyl protons on the ring carbon at 0.16 ppm couple with the silicon atom at 2.4 ppm. These results are wholly consistent with the structure proposed for the product **8**.

Furthermore, the results obtained from NOE-FID difference experiments at 300 MHz are also consistent with the structure proposed for **8**. Thus, irradiation of a signal at −0.16 ppm, due to the trimethylsiloxy protons on the ring silicon atom, reveals a strong enhancement of the signal at −0.07 ppm, attributed to the trimethylsilyl protons on the ring silicon atom, and the signals at 2.11 and 2.28 ppm, due to two methyl protons of the mesityl group, as well as the aromatic protons. Saturation of a signal at −0.07 ppm, due to the trimethylsilyl protons on the ring silicon atom, results in a positive NOE of the trimethylsiloxy and trimethylsilyl protons at −0.16 and 0.16 ppm and the phenyl ring protons. Irradiation of the trimethylsilyl protons at 0.16 ppm on the ring carbon atom leads to enhancement of the trimethylsilyl protons on the ring silicon atom at −0.07 ppm and two differet kinds of methyl protons of the mesityl group at 2.11 and 2.28 ppm, as well as the phenyl ring protons. Saturation of the methyl protons of the mesityl group at 2.28 ppm results in a strong enhancement of the trimethylsiloxy

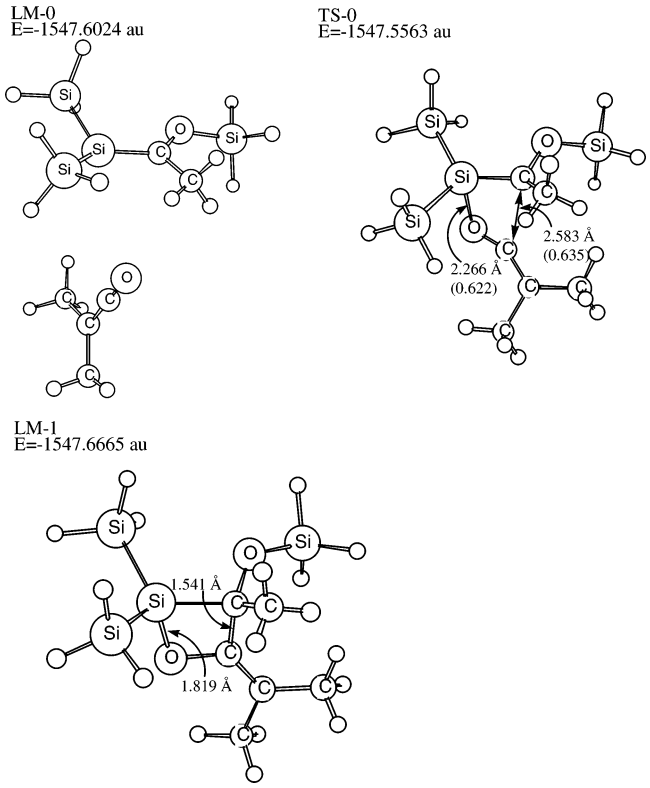

Figure 2. Optimized structures of the reactant, TS, and product with the simplified models for addition of silene to $(CH_3)_2C{=}C{=}O$. Some typical bond lengths are shown. The numbers in parentheses indicate the weight of that bond length in the reaction coordinate at TS.

protons on the ring silicon atom and the trimethylsilyl protons on the ring carbon atom, in addition to the mesityl ring protons. The formation of **8** may be explained in terms of a 1,2-trimethylsilyl shift with high stereospecificity from oxygen to the ring carbon atom in $\mathbf{A_3}$, simultaneously with ring expansion to the *cis*-2-siloxetane derivative. Unfortunately, the direct evidence for the formation of the intermediate $\mathbf{A_3}$ has not yet been obtained at present. However, for the stereospecific formation of the silacyclopropane $\mathbf{A_3}$, some through-space interaction between the oxygen in a trimethylsiloxy group and the trimethylsilyl silicon atom located on the same side of the silacyclopropane ring might be present.[3d]

Theoretical Calculations. To clarify the mechanism for a series of isomerizations of the [2 + 2] cycloadducts derived from the reaction of **1**−**3** with diphenylketene, to the products **6**−**8**, via the intermediates $\mathbf{A_{1-3}}$, we have carried out the density functional theory (DFT) calculations using the Gaussian03 program package.[7] The Becke three-parameter Lee−Yang−Parr

(7) Frisch, M. J.; Trucks, G. W.; Schlegel, H. B.; Scuseria, G. E.; Robb, M. A.; Cheeseman, J. R.; Montgomery, J. A., Jr.; Vreven, T.; Kudin, K. N.; Burant, J. C.; Millam, J. M.; Iyengar, S. S.; Tomasi, J.; Barone, V.; Mennucci, B.; Cossi, M.; Scalmani, G.; Rega, N.; Petersson, G. A.; Nakatsuji, H.; Hada, M.; Ehara, M.; Toyota, K.; Fukuda, R.; Hasegawa, J.; Ishida, M.; Nakajima, T.; Honda, Y.; Kitao, O.; Nakai, H.; Klene, M.; Li, X.; Knox, J. E.; Hratchian, H. P.; Cross, J. B.; Adamo, C.; Jaramillo, J.; Gomperts, R.; Stratmann, R. E.; Yazyev, O.; Austin, A. J.; Cammi, R.; Pomelli, C.; Ochterski, J. W.; Ayala, P. Y.; Morokuma, K.; Voth, G. A.; Salvador, P.; Dannenberg, J. J.; Zakrzewski, V. G.; Dapprich, S.; Daniels, A. D.; Strain, M. C.; Farkas, O.; Malick, D. K.; Rabuck, A. D.; Raghavachari, K.; Foresman, J. B.; Ortiz, J. V.; Cui, Q.; Baboul, A. G.; Clifford, S.; Cioslowski, J.; Stefanov, B. B.; Liu, G.; Liashenko, A.; Piskorz, P.; Komaromi, I.; Martin, R. L.; Fox, D. J.; Keith, T.; Al-Laham, M. A.; Peng, C. Y.; Nanayakkara, A.; Challacombe, M.; Gill, P. M. W.; Johnson, B.; Chen, W.; Wong, M. W.; Gonzalez, C.; Pople, J. A. *Gaussian 03*, Revision B.03; Gaussian, Inc.: Pittsburgh, PA, 2003.

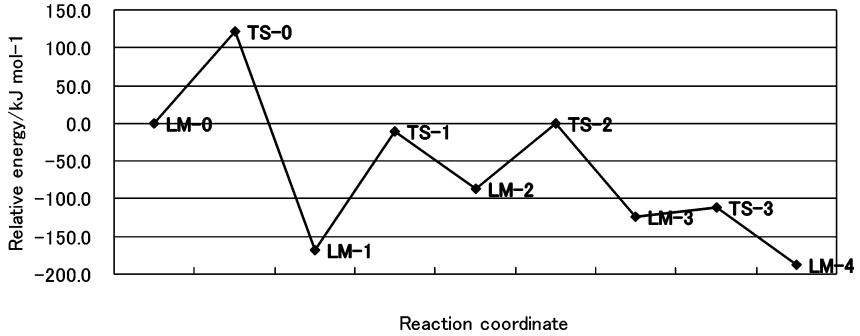

Figure 3. Energy change along with addition of **4** to $(CH_3)_2C{=}C{=}O$ (LM-0 to LM-1) and the formation of the three-membered ring (LM-1 to LM-4) with the simplified models.

hybrid functional[8−11] was employed with the 6-31G basis set. Two types of models, i.e., real and simplified, are used. In the real models, the substituents are the same as those used in the experiments, whereas in the simplified models, all methyl groups are replaced by hydrogen atoms and the phenyl groups originated from diphenylketene are substituted for the methyl groups. For the transformation of silacyclopropanes $\mathbf{A_{1,2}}$ to disilacyclobutanes $\mathbf{B_{1,2}}$ and $\mathbf{A_3}$ to siloxetane **8**, the trimethylsilyl groups are employed even in the simplified models, because migration of a methyl moiety in this group is involved during the isomerization reaction. Therefore, in these models, there are no structural differences among the intermediates $\mathbf{A_1}$, $\mathbf{A_2}$, and $\mathbf{A_3}$, which have the *tert*-butyl, adamantyl, and mesityl group, respectively.

Calculations are carried out as follows: (1) the transition states (TSs) on the potential energy surface are characterized by using the simplified models; (2) the intrinsic reaction coordinate (IRC) analysis is carried out at each TS for both directions, i.e., reactant and product sides. To save calculation time, the IRC analysis is restricted in the neighborhood of the TS, and full optimization is carried out at the end point of the IRC analysis. Thus, two local minima (LMs) are located in the reactant and product sides. (3) For the reaction paths from $\mathbf{A_1}$ to $\mathbf{B_1}$ and from $\mathbf{A_3}$ to **8**, the energies of all the LMs and TSs are evaluated again using the real models.

The pathways from the reaction of acylpolysilanes **1**−**3** with diphenylketene, leading to disilacyclobutanes $\mathbf{B_{1,2}}$ and siloxetane **8**, via silacyclopropanes $\mathbf{A_{1-3}}$, were divided into three parts, i.e., addition of the silenes to the ketene, ring contraction of the siloxetanes thus formed to the silacyclopropanes $\mathbf{A_{1-3}}$, and isomerization of $\mathbf{A_{1,2}}$ to $\mathbf{B_{1,2}}$ and $\mathbf{A_3}$ to **8**, respectively.

Addition of Silene to Ketene. We first examined the reaction of the simplified silene with dimethylketene, leading to a formal [2 + 2] cycloadduct, siloxetane (LM-1). LM-0 consists of isolated silene and dimethylketene, and its energy is taken as a standard. The optimized structures for LM-0, TS-0, and LM-1 are shown in Figure 2. The energy changes for this reaction are also shown in Figure 3. The energy of TS-0 was calculated to be more unstable by 121 kJ/mol than that of LM-0, while the siloxetane LM-1 is more stable than LM-0 by 168 kJ/mol. This result indicates that the formal [2 + 2] cycloadducts, siloxetanes, may be produced as the intermediates in the thermal reaction of **1**−**3** with diphenylketene, in contrast to the reaction of the silenes generated from **1** and **2** with trimethylsilylketene reported by Brook and Baumegger.[6]

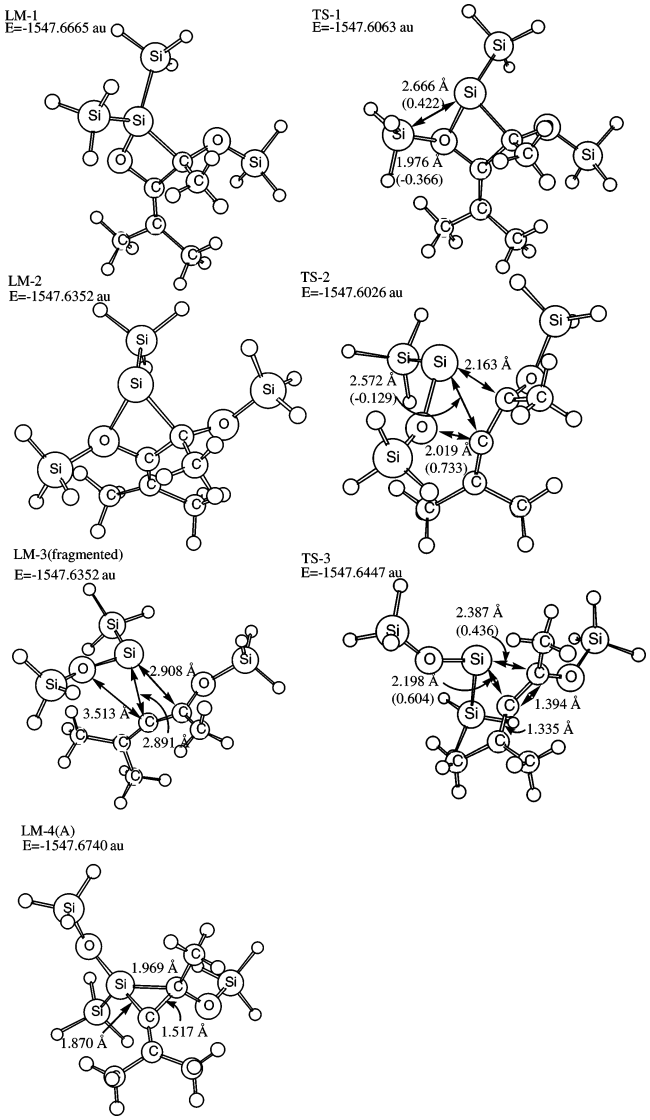

Figure 4. Optimized structures of the simplified models, LM-1, TS-1, LM-2, TS-2, LM-3, TS-3, and LM-4(A). See the caption of Figure 2 for the numbers.

Ring Contraction of LM-1 to Simplified Silacyclopropane A. The optimized geometries of the LMs and TSs, which are involved in the transformation of LM-1 to the silacyclopropane **A**, are shown in Figure 4. TS-1 represents a 1,2-H_3Si shift from the ring silicon to the oxygen in siloxetane LM-1, to give a four-membered cyclic intermediate (LM-2). TS-2 indicates scission of two bonds, Si−C and O−C, in the four-membered ring of LM-2, to give two fragments, siloxysilylsilylene (H_3-SiO(H_3Si)Si:) and siloxypropadiene. LM-3 is characterized as

(8) Becke, A. D. *Phys. Rev. A* **1988**, *38*, 3098.
(9) Lee, C.; Yang, W.; Parr, R. G. *Phys. Rev. B* **1988**, *37*, 785.
(10) Becke, A. D. *J. Chem. Phys.* **1993**, *98*, 1372.
(11) Gill, P. M. W.; Johnson, B. G.; Pople, J. A. *Int. J. Quantum Chem. Symp.* **1992**, *26*, 319.

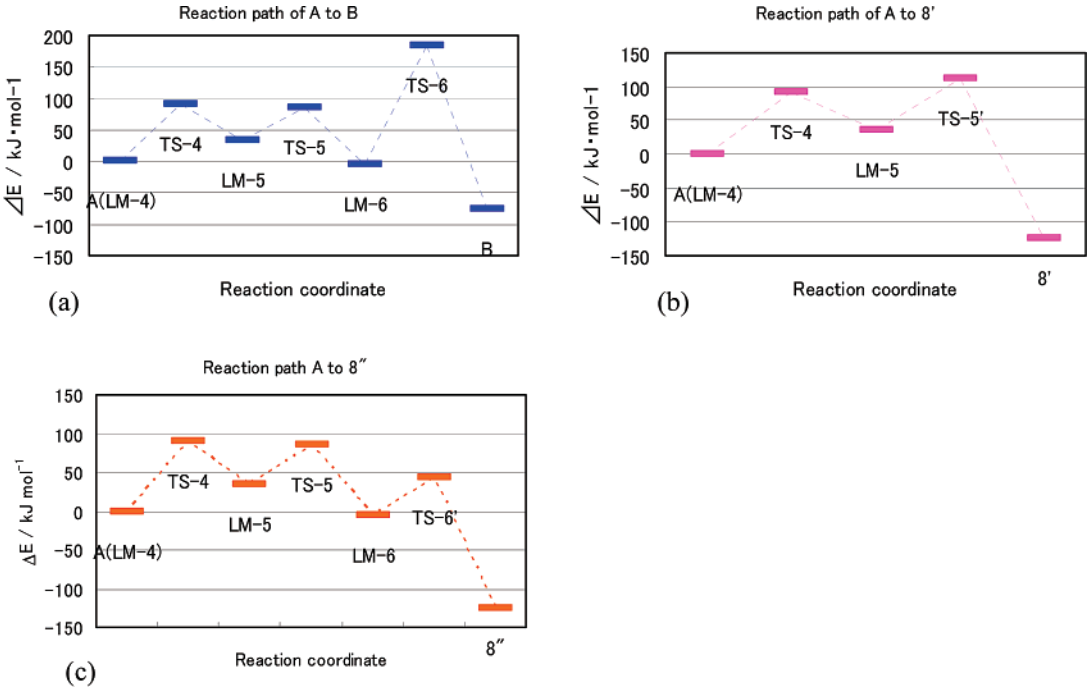

Figure 5. Energy change along **A** to **B**, **A** to **8′**, and **A** to **8″** with simplified models. Both **8′** and **8″** indicate the simplified model for **8**. (a) The path to **B**; (b) one possible path to **8′**, where **A** (LM-4) to LM-5 is the same as the path to **B**; (c) another possible path to **8″**, where **A** (LM-4) to LM-6 is the same as the path to **B**.

the intermediate in which these two fragment molecules are loosely binding each other. Addition of siloxysilylsilylene to the carbon−carbon double bond in the propadiene produces silacyclopropane (LM-4), which corresponds to **A**. We confirmed by the intrinsic reaction coordinate (IRC) analysis that TS-2 connects to LM-2 and LM-3, TS-3 connects to LM-3 and LM-4, and the geometry for LM-3 included in both analyses is identical, which means a single reaction path from LM-2 toward LM-4. The energy changes along the reaction course are also shown in Figure 3. Compared with the energy changes from LM-0 to LM-1, those from TS-1 to LM-4 are relatively flat and practically downhill, showing that splitting of the siloxetane into siloxysilylsilylene and propadiene and recombination of these two fragments readily take place.

Ring Enlargement of $A_{1,2}$ to $B_{1,2}$ and A_3 to 8. The energy profiles with the simplified models are shown in Figure 5. Isomerization of silacyclopropane LM-4 to disilacyclobutane **B** proceeds through TS-4, LM-5, TS-5, LM-6, and TS-6. For the isomerization of $\mathbf{A_3}$ to **8**, two simplified models, **8′** and **8″**, are produced for the ring enlargement of LM-4. The structures for **8′** and **8″** differ only by the location of the $Si(CH_3)_3$ group, and this difference does not occur for the real models. One involves the intermediates TS-4, LM-5, and TS-5′, and the other involves TS-4, LM-5, TS-5, LM-6, and TS-6′. The geometries for LM-4, TS-4, LM-5, TS-5, and LM-6 are common in all three pathways. Along the reaction path from LM-4 to **B**, the energy of TS-6 is the highest, and the activation energy, which is a relative energy for TS-6 with respect to LM-4, is calculated to be 183 kJ/mol. In the two different pathways starting from LM-4, leading to **8′** and **8″**, the highest energies are located at TS-5′ and TS-4, respectively. Since the energy of TS-5′ is higher than that of TS-4, and the energy of TS-6′ is lower than those of TS-4 and TS-5, their activation energies are estimated to be 111 and 91 kJ/mol, respectively. Thus, in either pathway for the transformation of LM-4 to **8′** or **8″**, the activation energy is smaller than that for isomerization of LM-4 to **B**. For the pathways leading to **8′** and **8″**, the activation energy in the reaction through TS-4, LM-5, TS-5, LM-6, and TS-6′ is smaller than that in the pathway involving TS-4, LM-5, and TS-5′. The optimized structures for LM-4, TS-4, LM-5, TS-5, LM-6, TS-6, and **B** are shown in Figure 6. TS-4 represents the ring-opening of LM-4 and a 1,2-Me_3Si shift from the Si atom to the C atom through TS-5, while TS-6 represents a methyl shift from the Me_3Si group onto the adjacent Si atom, to give the disilacyclobutane derivative.

The optimized geometries for TS-5′, TS-6′, **8′**, and **8″** are shown in Figure 7. TS-5′ branches off from LM-5 and describes the formation of the Si−O bond leading to the four-membered ring. The IRC and successive optimization show the migration of the SiH_3 group on the oxygen atom to the adjacent C atom and the formation of **8′**. TS-6′ branches off from LM-6 and indicates the attack of the oxygen atom in the $O-SiH_3$ group onto the siloxy-substituted Si atom, to give the four-membered ring, followed by migration of the SiH_3 group on the oxygen atom to the adjacent Si atom, to afford **8″**.

The energies of individual LMs and TSs were evaluated again using the real models with *tert*-butyl substituent. The energy profile for the isomerization of $\mathbf{A_1}$ to **B** is shown in Figure 8a. The energies for LM-4(A_1), LM-5, TS-5, LM-6, TS-6, and **B** are plotted as horizontal bars. In the real model calculation, TS-4 is not characterized. The essential structural change from LM-4 to LM-5 involves elongation of the $Si-C(OSiMe_3)$ bond, followed by ring-opening of the silacyclopropane derivative. The geometries of the five intermediates are generated at a 0.1 Å increment of the Si−C bond lengths, and they are optimized with respect to the other internal parameters. Those energies are also plotted in Figure 8a. The energy change is very small, and the TS seems to be absent. TS-6 shows again the highest energy for the model with a *tert*-butyl substituent.

For the reaction from $\mathbf{A_3}$ to **8**, the structures and energies are evaluated only for the second reaction path using the real models with a mesitylene substituent. Figure 8b shows the energies for LM-4(A_3), LM-5, TS-5, LM-6, TS-6′, and **8**, as well as those for the structures of the six intermediates, lying between LM-4

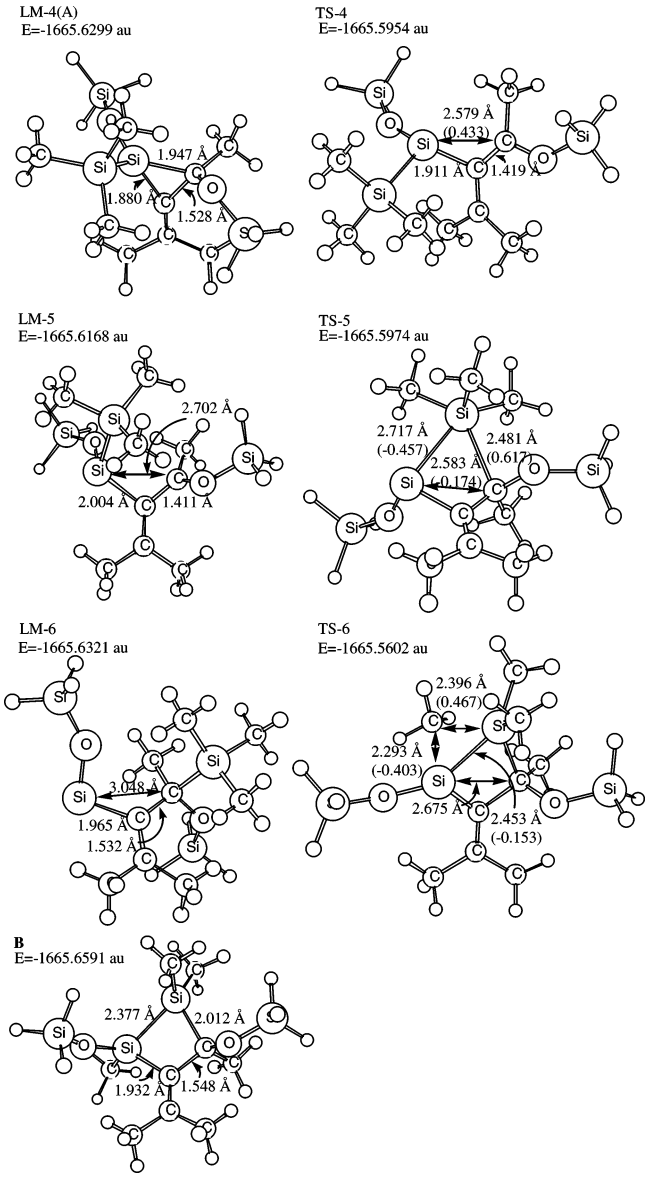

Figure 6. Optimized structures of the simplified models, LM-4(A), TS-4, LM-5, TS-5, LM-6, TS-6, and **B**. The structure of LM-4(A) is different from that shown in Figure 4 with respect to the Si−Si$(CH_3)_3$ moiety in place of Si−SiH_3. However the same label is used for simplicity. See the caption of Figure 2 for the numbers.

and LM-5, as plotted by horizontal bars. The real model calculations indicate that the energy of TS-6′ is higher than that of TS-4 obtained from the simplified model.

To learn more about the difference in the reactions between the *tert*-butyl and mesitylene substituent, we carried out the calculations using the real models. The TS-6 structure for the transformation of $\mathbf{A_1}$ to **B** was characterized using a compound bearing the mesitylene substituent, and the energy is plotted in Figure 8b as a square. On the contrary, the TS-6′ structure for the isomerization of $\mathbf{A_3}$ to **8** was characterized with the *tert*-butyl substituent, and the energy is plotted as a square in Figure 8a. As can be seen in Figure 8a, the energy of TS-6′ is lower than that of TS-6. This means that the reaction of $\mathbf{A_1}$ leading to **8** occurs more easily than that of $\mathbf{A_1}$ to **B**, which is inconsistent with the experimental results. On the other hand, the energy of TS-6′ is again lower than that of TS-6, as shown in Figure 8b. This means that the reaction of $\mathbf{A_3}$ to **8** occurs more easily than that of $\mathbf{A_3}$ to **B**, which is consistent with the experimental results. Thus, the present calculations conclude that the reaction leading

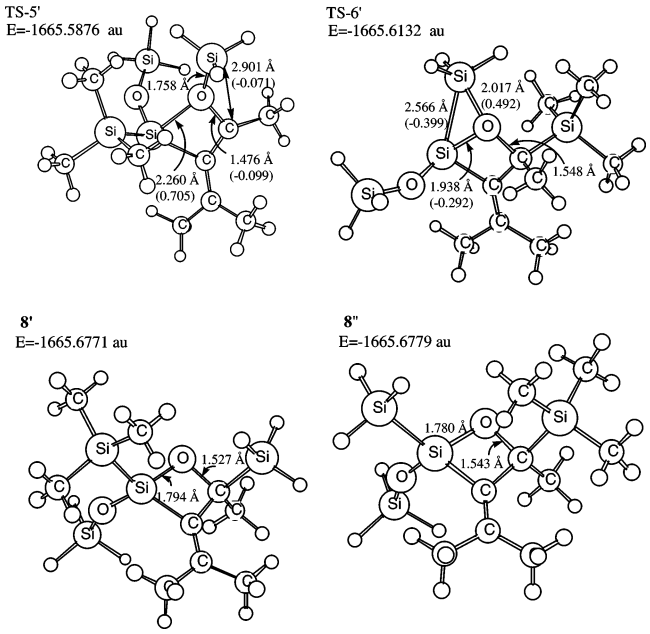

Figure 7. Optimized structures of simplified models TS-5′, TS-6′, **8**′, and **8**″. See the caption of Figure 2 for the numbers.

to **8** proceeds more easily regardless of the substituents. This trend seems to be suggested even in the energy of the simplified models shown in Figure 5. Although the present calculation did not reproduce completely the experimental findings, detailed information on the reaction mechanism including the TS structures was obtained. The change of the reaction profile due to variation of the bulky substituents at the periphery of molecules is often found in the experiments. However, its theoretical explanation still seems to be a difficult subject for the current level of calculation.

X-ray Crystallographic Analysis for Compound 6. Cell dimensions, data collection and refinement parameters, and selected bond lengths and angles for **6** are summarized in Tables 1 and 2, and the ORTEP view is presented in Figure 1.

As can be seen in Figure 1, the four-membered silacyclobutene ring of **6** is almost planar, as indicated by the small torsion angle of Si1−C1−C2−C3 = 0.3(1)°, similar to other silacyclobutenes reported previously.[12−15] The small inner ring angle around silicon (C1−Si1−C3 = 76.58(7)°) and large C−C═C angle (106.2(1)°) also are general characteristics of the silacyclobutenes.

In conclusion, the co-thermolyses of acylpolysilanes **1** and **2** with diphenylketene afforded the 1-silacyclobut-2-ene derivatives **6** and **7**, respectively. Similar thermolysis of mesitoyltris(trimethylsilyl)silane **3** with diphenylketene, however, gave siloxetane **8**, which underwent thermolysis to give 1-mesityl-2,2-diphenyl-1-trimethylsilylpropadiene and trimethylsiloxy(trimethylsilyl)silanone. The results of the theoretical calculations indicated that the reactions of the silenes with ketene produce formal [2 + 2] cycloadducts, siloxetanes at the initial step, and the siloxetanes thus formed undergo successive isomerization to give the products **6**−**8**, in accord with the mechanism proposed.

(12) Ishikawa, M.; Sugisawa, H.; Akitomo, H.; Matsusaki, K; Kamitori, S.; Hirotsu, K.; Higuchi, T. *Organometallics* **1986**, *5*, 2447.
(13) Brook, A. G.; Baumegger, A.; Lough, A. J. *Organometallics* **1992**, *11*, 3088.
(14) Lassacher, P.; Brook, A. G.; Lough, A. J. *Organometallics* **1995**, *14*, 4359.
(15) Auner, N.; Grasmann, M.; Herrschaft, B.; Hummer, M. *Can. J. Chem.* **2000**, *78*, 1445.

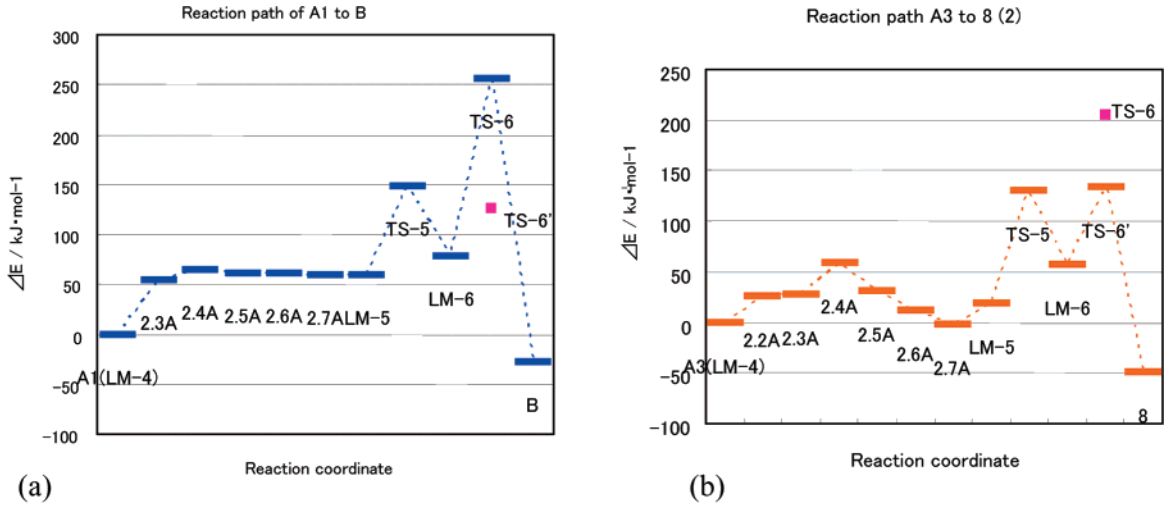

Figure 8. Energy change along **A** to **B** and **A** to **8** using the real models. (a) The path from $\mathbf{A_1}$ to **B**; (b) the path from $\mathbf{A_3}$ to **8**.

Table 1. Crystal Data, Experimental Conditions, and Summary of Structural Refinement for Compound 6

mol formula	$C_{28}H_{46}O_2Si_4$
mol wt	527.01
space group	$P\bar{1}$ (#2)
cell dimens	
a, Å	9.9222(3)
b, Å	10.0080(4)
c, Å	18.5846(8)
α, deg	98.864(2)
β, deg	95.544(1)
γ, deg	118.6237(9)
V, Å^3	1569.4(1)
Z	2
D_{cacld}, Mg/m^3	1.115
F(000)	572.00
cryst size, mm^3	0.4 × 0.1 × 0.1
cryst color	colorless
μ, cm^{-1}	2.11
radiation	Mo Kα (λ = 0.71069 Å)
temp, K	100
2*θ* max	54.8
no. of unique reflns	6936
no. of obsd reflns ($I \geq 3\sigma(I)$)	6483
reflns/params	18.37
corrections	Lorentz−polarization absorption
absorp range	0.9563−1.1271
R	0.034
R_w[a]	0.043

[a] Weighting scheme is $(\sigma(F_o)^2 + 0.0004|F_o|^2)^{-1}$.

Table 2. Selected Bond Distances (Å) and Angles (deg) for Compound 6 with Their esd's in Parentheses

Si1	C1	1.858(2)	Si1	C3	1.927(2)
Si1	C4	1.867(2)	Si1	C5	1.870(2)
Si2	C2	1.879(2)	C1	C2	1.363(2)
C1	C6	1.512(2)	C2	C3	1.566(2)
C3	C11	1.526(2)	C3	C17	1.519(2)

C1	Si1	C3	76.58(7)	C1	Si1	C4	115.76(8)
C3	Si1	C4	114.92(8)	C1	Si1	C5	119.32(8)
C3	Si1	C5	118.63(8)	C4	Si1	C5	108.84(9)
O1	Si2	O2	108.63(7)	O1	Si2	C2	110.49(8)
O2	Si2	C2	107.23(7)	O1	Si2	C10	108.24(8)
O2	Si2	C10	108.69(8)	C2	Si2	C10	113.45(8)
Si1	C1	C2	92.9(1)	Si1	C1	C6	134.0(1)
C2	C1	C6	132.9(2)	Si2	C2	C1	132.5(1)
Si2	C2	C3	121.2(1)	C1	C2	C3	106.2(1)
Si1	C3	C2	84.3(1)	Si1	C3	C11	118.9(1)
C2	C3	C11	110.2(1)	Si1	C3	C17	108.7(1)
C2	C3	C17	115.0(1)	C11	C3	C17	115.9(1)

Experimental Section

General Procedure. All thermal reactions of acylpolysilanes **1**−**3** with diphenylketene were carried out in a degassed sealed tube (1.0 cm × 15 cm). Yields of the products were calculated on the basis of the isolated products. NMR spectra were recorded on JNM-LA300 and JNM-LA500 spectrometers. Infrared spectra were recorded on a JEOL model JIR-DIAMOND 20 infrared spectrophotometer. Low- and high-resolution mass spectra were measured on a JEOL model JMS-700 instrument. Column chromatography was performed by using Wakogel C-300 (WAKO).

Materials. Acylpolysilanes **1**−**3** were prepared according to the method reported by Brook et al.[2]

Thermolysis of 1 with Diphenylketene. A mixture of 0.6100 g (1.83 mmol) of **1** and 0.4342 g (2.23 mmol) of diphenylketene was heated in a sealed glass tube at 140 °C for 24 h. The mixture was chromatographed on a silica gel column, with hexane as eluent, to give the product **6** (0.4238 g, 44% yield) and unchanged **1** (0.3050 g, 50%). The product **6** was recrystallized from ethanol. Anal. Calcd for $C_{28}H_{48}O_2Si_4$: C, 63.81; H, 8.80. Found: C, 63.77; H, 8.96. Mp: 88 °C. MS: *m*/*z* 526 (M^+). IR: 2954, 2900, 1490, 1257, 1074, 1045, 840, 790, 754, 709, 698 cm^{-1}. ^{1}H NMR *δ* ($CDCl_3$): −0.64 (s, 3H, MeSi), −0.03 (s, 6H, Me_2Si), 0.04 (s, 18H, Me_3Si), 1.21 (s, 9H, *t*-Bu), 7.06−7.32 (m, 10H, phenyl ring protons). ^{13}C NMR *δ* ($CDCl_3$): −0.42 (Me_2Si), 1.92 (Me_3Si), 2.38 (MeSi), 30.82 (Me_3C), 36.27 (CMe_3), 52.64 (CPh), 124.00, 127.45, 128.39, 144.85 (phenyl ring carbons), 158.14, 179.54 (olefinic carbons). ^{29}Si NMR *δ* ($CDCl_3$): −42.2, 6.6, 16.9.

Thermolysis of 2 with Diphenylketene. A mixture of 0.5130 g (1.25 mmol) of **2** and 0.2751 g (1.41 mmol) of diphenylketene was heated at 140 °C for 12 h. Product **7** (0.3775 g, 50% yield) was isolated by silica gel column chromatography eluting with hexane, along with the starting compound **2** (0.2052 g, 40%). The product **7** was purified by recrystallization from ethanol. Anal. Calcd for $C_{34}H_{52}O_2Si_4$: C, 67.49; H, 8.66. Found: C, 67.55; H, 8.67. Mp: 159 °C. MS: *m*/*z* 604 (M^+). IR: 2956, 2902, 2846, 1494, 1446, 1257, 1078, 1047, 838, 792, 754, 700 cm^{-1}. ^{1}H NMR *δ* ($CDCl_3$): −0.66 (s, 3H, MeSi), −0.03 (s, 6H, Me_2Si), 0.05 (s, 18H, Me_3Si), 1.52−1.99 (m, 15H, Ad), 7.05−7.33 (m, 10H, phenyl ring protons). ^{13}C NMR *δ* ($CDCl_3$): −0.12 (Me_2Si), 1.97 (Me_3Si), 2.04 (MeSi), 28.69, 36.91, 38.49, 42.57 (Ad), 53.00 (CPh), 123.95, 127.42, 128.39, 144.89 (phenyl ring carbons), 157.98, 179.61 (olefinic carbons). ^{29}Si NMR *δ* ($CDCl_3$): −42.4, 6.5, 17.2.

Thermolysis of 3 with Diphenylketene. A mixture of 0.6066 g (1.53 mmol) of **3** and 0.3830 g (1.97 mmol) of diphenylketene was heated at 160 °C for 24 h. The mixture was chromatographed on a silica gel column with hexane as eluent, to give the product **8** (0.4009 g, 44% yield) and the starting compound **3** (0.1049 g, 17%).

The product **8** was purified by recrystallization from ethanol. Anal. Calcd for $C_{33}H_{48}O_2Si_4$: C, 67.28; H, 8.21. Found: C, 67.29; H, 8.15. Mp: 125 °C. MS: *m*/*z* 588 (M^+). IR: 3052, 3016, 2954, 2898, 1594, 1494, 1473, 1440, 1249, 1087, 1072, 1047, 933, 840, 754, 694 cm^{-1}. ^1H NMR δ ($CDCl_3$): −0.16 (s, 9H, Me_3Si), −0.07 (s, 9H, Me_3Si), 0.16 (s, 9H, Me_3Si), 2.11 (s, 3H, Me−Ar), 2.19 (s, 3H, Me−Ar), 2.28 (s, 3H, Me−Ar), 6.69 (s, 2H, H−Ar), 7.15−7.30 (m, 8H, phenyl ring protons), 7.56 (d, 2H, phenyl ring protons, J = 8.2 Hz). ^{13}C NMR δ ($CDCl_3$): −1.46, −0.94, 1.10 (Me_3Si), 20.45, 21.72, 23.65 (Me−Ar), 96.68 (CO), 125.84, 126.16, 127.64, 128.22, 128.93, 129.36, 129.40, 130.90, 131.88, 133.12, 135.72, 138.36, 141.38, 168.30 (phenyl and mesityl ring and olefinic carbons). ^{29}Si NMR δ ($CDCl_3$): −19.1, 2.4, 2.6, 11.8.

Thermolysis of Siloxetane 8. A solution of 0.1005 g (0.171 mmol) of **8** in 0.25 mL of dry benzene was heated at 200 °C for 24 h. A 1-trimethylsiloxypropadiene derivative (0.0283 g, 43% yield) was isolated by silica gel column chromatography. Anal. Calcd for $C_{27}H_{30}Si$: C, 84.76; H, 7.90. Found: C, 84.77; H, 7.70. MS: *m*/*z* 382 (M^+). IR: 2954, 2921, 2852, 1909, 1741, 1596, 1492, 1450, 1249, 879, 838, 765, 694 cm^{-1}. ^1H NMR δ ($CDCl_3$): 0.18 (s, 9H, Me_3Si), 2.20 (s, 6H, Me−Ar), 2.26 (s, 3H, Me−Ar), 6.85 (s, 2H, H−Ar), 7.21−7.32 (m, 10H, phenyl ring protons). ^{13}C NMR δ ($CDCl_3$): −0.19 (Me_3Si), 20.85, 21.39 (Me−Ar), 101.41, 103.66 (allene carbons), 126.51, 128.25, 128.28, 128.36, 133.23, 135.02, 135.21, 137.15 (phenyl and mesityl ring). ^{29}Si NMR δ ($CDCl_3$): −0.7.

X-ray Crystallographic Analysis. Data collection was performed on a Rigaku RAXIS-RAPID imaging plate system. The structures were solved by direct methods[16] and expanded using Fourier techniques.[17] The non-hydrogen atoms were refined anisotropically. Hydrogen atoms were included but not refined. All calculations were performed using the Crystal Structure crystallographic software package.[18,19]

Acknowledgment. This work was supported by a Grant-in-Aid for Scientific Research (No. 14750687 and 15550038) from the Ministry of Education, Science, Sports and Culture of Japan, to which our thanks are due. We thank Sumitomo Chemical Co., Ltd. for financial support. We also thank Shin-Etsu Co., Ltd. for the gift of chlorosilanes.

Supporting Information Available: Crystallographic data as a CIF file for **6**. This material is available free of charge via Internet at http://pubs.acs.org.

OM700838N

(16) SHELEX86 was used for **4**: Sheldrick, D. M. *Program for the solution of crystal structures*; University of Gottingen, Germany. SIR92 was used for **7**: Altomare, A.; Cascarano, G.; Giacovazzo, C.; Guagliardi, A.; Burla, M.; Polidori, G.; Camalli, M. *J. Appl. Crystallogr*. **1994**, *27*, 435.

(17) DIRDIF99: Beurskens, P. T.; Admiraal, G.; Bosman, W. P.; de Gelder, R.; Israel, R.; Smits, J. M. M. *The DIRDIF-99 program system*, Technical Report of the Crystallography Laboratory; University of Nijmegen: The Netherlands, 1999.

(18) *Crystal Structure 3.10*, Crystal Structure Analysis Package; Rigaku and Rigaku/MSC, 2000−2002.

(19) Watkin, D. J.; Prout, C. K.; Carruthers, J. R.; Betteridge, P. W. *CRYSTALS Issue 10*; Chemical Crystallography Laboratory: Oxford, UK, 1996.